JOURNAL OF APPLIED ELECTROCHEMISTRY **27** (1997) 815–820

# Scanning probe microscopy studies of Ebonex® electrodes

J. R. SMITH*

*Scanning Probe Microscopy Laboratory, School of Pharmacy, Biomedical and Physical Sciences, University of Portsmouth, PO1 2DT, Great Britain*

A. H. NAHLÉ‡, and F. C. WALSH

*Applied Electrochemistry Group, School of Pharmacy, Biomedical and Physical Sciences, University of Portsmouth, St. Michael's Building, White Swan Road, Portsmouth, PO1 2DT, Great Britain*

Received 20 August 1996; revised 16 January 1997

The porosity of Ebonex® electrodes is known to have a marked affect on their electrochemical properties. Atomic force microscopy (AFM) and scanning tunnelling microscopy (STM) have been used to investigate the topography of porous and fully-hardened (nonporous) Ebonex® at high resolution. AFM has also been used to study the early stages of copper electrodeposition on porous Ebonex® electrodes. Initial copper nucleation and growth were found to occur preferentially at surface pores.

## 1. Introduction

Ebonex®, a composition of substoichiometric oxides of titanium (Magnéli phases), of the general formula $Ti_nO_{2n-1}$, where $n$ is in the range 4–10 [1], is attracting increasing attention as a novel electrode material [2–4]. Ebonex® is produced by heating titanium dioxide (rutile, $TiO_2$) to temperatures exceeding 1200 °C followed by cooling to ambient temperature under an atmosphere of hydrogen [3]. The porosity of the ceramic material produced can be controlled by the composition of $TiO_2$ powder together with the control of sintering and reducing conditions during processing [5].

Ebonex® is an attractive material for the fabrication of electrodes for a diverse range of technological applications, such as chlorine generation, sodium chlorate production, battery materials and impressed current cathodic protection systems [6–8]. It can also be readily coated with catalytic materials, such as $PbO_2$ for ozone generation [4] and $RuO_2$ for oxygen evolution [9]. The latter coating has also been proposed as a suitable electrode for hydrogen evolution from human faeces and urine in spacecraft [10], utilizing bacteria and electrochemical incineration of the wastes to produce $CO_2$ and $N_2$ with $H_2$ as the cathodic product. The hydrogen produced is a clean fuel which does not contain hydrocarbon combustion products. $Ru–Ti_4O_7$ has also been used as a microelectrode for the oxidation of $I^-$ to $I_2$ and $IO_3^-$ in 0.1 mol dm$^{-3}$ $H_2SO_4$ [11].

Ebonex® can be fabricated or shaped into a variety of forms to produce electrodes of complex geometry having a good chemical resistance. The ceramic material has a greater resistance to aggressive environments than many conventional electrode materials. In addition, it can be used in anodic, cathodic, bipolar and polarity switching operations owing to chemical inertness in both oxidizing and reducing conditions. The high overpotential required for hydrogen and oxygen evolution [12] makes the material suitable for the cathodic deposition of metals, such as copper, gold, nickel, palladium and platinum, which can adhere strongly to Ebonex® surfaces [3].

The porosity of Ebonex® electrodes has been shown to have a marked affect on their electrochemical behaviour [5], with the shape of the cyclic voltammogram (CV) and the potentials for the oxygen and hydrogen evolution reactions being strongly dependent on pore size distribution in the ceramic electrodes. For example, the onset of the oxygen evolution reaction has been shown to increase from +2.5 V vs SCE to +2.8 V vs SCE on going from a material containing many large pores to one containing a small number of small pores. In addition, it has been reported that the most reproducible CVs and largest current densities are displayed by electrodes containing many large pores [5].

Preliminary microscopic characterization of porous Ebonex® surfaces has been carried out using scanning electron microscopy (SEM) [3]. Electrodeposition of a 1 $\mu$m thick layer of copper has been shown to produce crystallites of copper within the pores. Thicker deposits, of about 50 $\mu$m, involved crystallites which had completely overlapped to form a continuous film [3]. Energy dispersive X-ray anal-

* Author to whom correspondence should be addressed.
‡ On study leave from: Department of Chemistry, Faculty of Arts and Sciences, The American University of Beirut, Beirut, The Lebanon.

0021-891X  

ysis of a cross-section showed that copper deposition occurred deep inside the pores of the material [3]. Here, atomic force microscopy (AFM) and scanning tunnelling microscopy (STM) have been used to characterize porous and fully-hardened (nonporous) Ebonex® electrodes [13–15].

## 2. Experimental details

Ebonex® tiles from two sources were used in the current study. The first was a porous tile (~ 15% porosity) obtained from Electrochemical Design Associates Ltd, London, UK, measuring 128 mm × 64 mm × 3.2 mm and the second, a fully-hardened (nonporous) tile from Atraverda Ltd, Sheffield, UK, measuring 60 mm × 40 mm × 2 mm. The physical properties of these materials are shown in Table 1. Both tiles were broken into 11 mm × 11 mm square tiles using a diamond-cutter as a guide and polished, initially with decreasing grades of emery paper, followed by alumina/distilled water slurries (of $Al_2O_3$ particle diameters: 7, 0.3 and 0.05 $\mu$m). The tiles were rinsed in chromic acid solution for about 10 s to remove any residual alumina, and then with double-distilled water and ethanol. The prepared surfaces appeared almost mirror-like, although some mottled features could be seen when very closely examined by the naked eye.

Copper(II) sulfate-pentahydrate (Fluka, puriss), sodium sulfate (BDH, GPR grade) and concentrated sulfuric acid (BDH, Aristar) were used 'as received'. A 1 mmol dm$^{-3}$ $Cu^{2+}$ solution in 0.1 mol dm$^{-3}$ $Na_2SO_4$/double distilled water was acidified to pH 2.0 by the addition of concentrated sulfuric acid. pH adjustments were monitored on a Corning model 150 pH meter with a BDH Gelplar combination electrode.

Ebonex® ceramic electrodes were constructed from 11 mm × 11 mm square plates of Ebonex® connected to copper wires using a silver-loaded epoxy cement (RS Components, 555-673). The assemblies were then encapsulated in glass tubes using epoxy cement (RS Components, 555-077) and polished prior to electrochemical experiments.

A Hi-Tek DT 2101 potentiostat coupled to a Hi-Tek PPR1 waveform generator was used to generate electrochemical data. Copper was electrodeposited onto stationary Ebonex® electrodes under potentiodynamic conditions. The potential was initially maintained at +0.20 V vs SCE, corresponding to oxygen evolution, to clean the electrode surface, and was then swept to −0.40 V vs SCE, corresponding to the onset of copper deposition, for varying time intervals. Three samples, A, B and C, possessing nominal film thicknesses of 1, 100 and 1000 monolayers, after the passage of charge for 0.086, 8.7 and 87 s, respectively, were prepared in this way. A thicker deposit of 0.06 $\mu$m, obtained after deposition at a potential of −0.40 V vs SCE for 56 min (sample D), was also prepared.

*Table 1. Some physical properties of Ebonex® electrodes used in the current study*

| | *Ebonex® sample* | |
|---|---|---|
| | *Fully-hardened (nonporous)* | *Porous* |
| Density/g cm$^{-3}$ | 4.35 | 8.84 |
| Porosity/% | 1–2 | 12–15 |
| Resistivity/$\mu\Omega$ cm | 3200 | 6600 |

Atomic force microscopy (AFM) and scanning tunnelling microscopy (STM) studies were performed in air under normal atmospheric conditions using a Discoverer TopoMetrix TMX2000 scanning probe microscope (SPM) instrument (TopoMetrix Corporation, Saffron Waldon, UK). For AFM studies, scanners capable of maximum $X$–$Y$ translations of 70 $\mu$m × 70 $\mu$m and 7 $\mu$m × 7 $\mu$m were used and imaging was performed in contact and noncontact mode using forces in the range of 1 to 20 nN. Standard profile pyramidal silicon nitride tips mounted on cantilevers of spring constant 0.036 N m$^{-1}$ were used for contact mode imaging. For some studies, a Supertip® (TopoMetrix Corporation, Santa Clara, CA, USA), consisting of a 1 $\mu$m long fine diamond-like needle at the end of a standard profile AFM tip, was used for contact mode imaging. For noncontact operation, silicon tips, mounted on cantilevers of the same material, were used and imaging recorded at the cantilevers natural resonant frequency of 209 Hz. For STM studies, a scanner capable of maximum $X$–$Y$ translation of 25 $\mu$m × 25 $\mu$m was used and images were obtained using a tip bias potential of 5 mV (sample at 0 V). STM tips were prepared from high-purity tungsten wire (0.25 mm diameter, 99.95%; Goodfellow, Cambridge, UK) electrochemically etched to a fine point in 2 mol dm$^{-3}$ KOH, as described elsewhere [16]. Quantitative data, such as height measurements, surface roughness and porosity, were obtained using TopoMetrix image analysis software [17]. Arithmetic surface roughness average $R_a$, is the arithmetic average of the absolute values of the measured profile height deviations, given by

$$R_a = \frac{1}{n}\sum_{i=1}^{n} |Z_i - \bar{Z}| \qquad (1)$$

where, $n$ = number of height positions along line profile, $Z_i$ = height at position $i$ (nm), and $\bar{Z}$ = average height (nm). For this study, 25 line profiles of 8.75 $\mu$m were measured for each image; the average $R_a$ value and its standard deviation were recorded.

## 3. Results and discussion

AFM images of porous and fully-hardened (nonporous) Ebonex® electrodes, obtained in contact mode, are shown in Fig. 1(a) and (b), respectively. Differences in topography between these two materials can clearly be observed. Pores in the porous tile were uniformly distributed over the surface, as might be

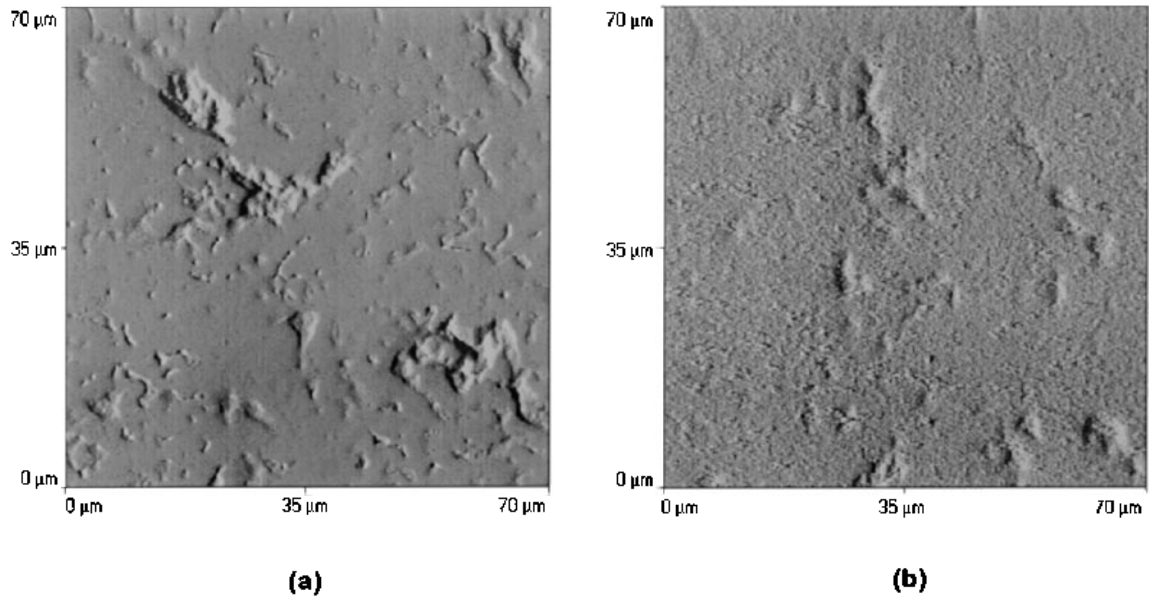


Fig. 1. AFM (contact mode) images of (a) porous and (b) 'fully-hardened' (non-porous) Ebonex® obtained using a standard profile AFM tip. Scan rate 140 $\mu m\,s^{-1}$.

expected from the prereduction treatment of the material during production. Contact mode AFM images of the 'fully-hardened' tile showed the material to be essentially non-porous, although some very shallow micropits ($< 1\,\mu$m in depth) were observed, consistent with SEM studies [3]. The surface appeared rougher than the porous tile (arithmetic surface roughness average, $R_a = 35 \pm 8$ nm, compared with $19 \pm 11$ nm for the porous material. This may be explained in terms of differences in hardness, where the softer porous tile can be more easily polished to a smoother finish.

Sections through the porous tile showed pit depths of 1–2 $\mu$m, as shown in Fig. 2. However, the upper-limit of pit depth may have been influenced by the inability of the wide pyramidal-shaped tip to probe the base of these pits. This is supported by the angular-shaped appearance of pore side-walls compared with images of those obtained from SEM studies [3].

To investigate the extent of these tip artefacts, the porous tile was rescanned using a 1 $\mu$m long Supertip®. This was expected to facilitate deeper probing of pores and a significant reduction in the number of artefacts caused by tip edges contacting pore-walls. The image shows a slight improvement in pore-shape compared with those obtained using the standard profile tip (Fig. 1(a)), although the tip was still unable to probe some of the deeper pores.

The surface porosity, defined as the ratio of the pore area to that of the projected image area [18], that is, in this case, 4900 $\mu m^2$, of the Ebonex® electrodes could readily be calculated using the TopoMetrix image analysis software [17]. Porosities of between 12% and 15% were obtained for the porous Ebonex®

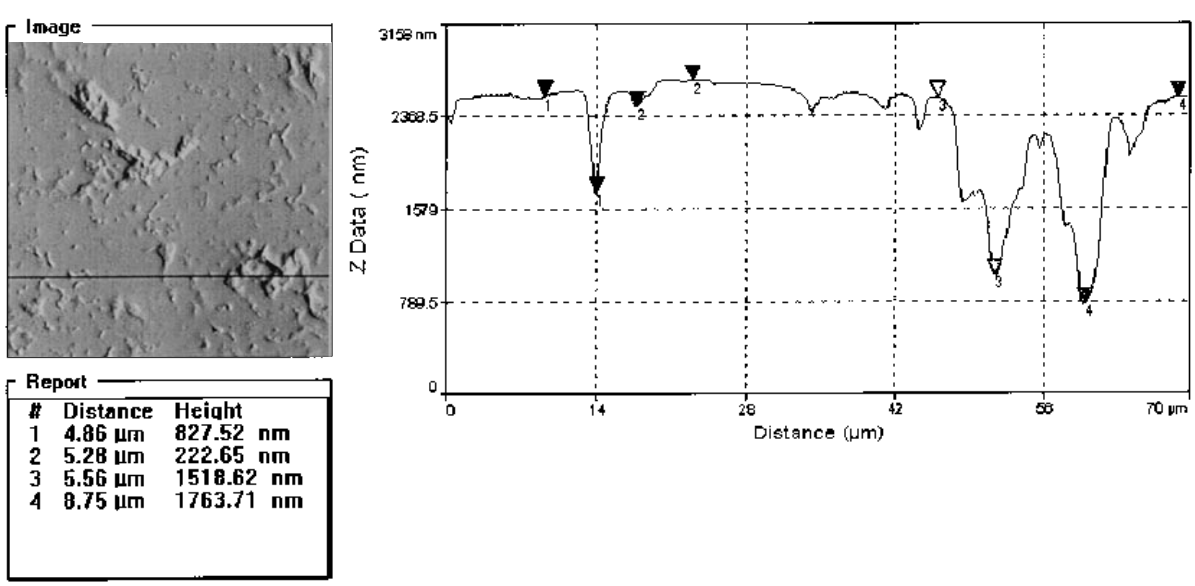


Fig. 2. Line section through the AFM image of porous Ebonex® (Fig. 1(a)), showing typical pore depths.

tile, in agreement with values ranging from 10% and 20% [19] determined from water immersion techniques (as quoted by manufacturers) [20]. Values of between 2% and 3% were obtained for the fully-hardened material, consistent with SEM porosity studies [3]. AFM provides a very rapid and useful method of porosity characterization and, in contrast to immersion techniques, provides detailed information on surface morphology.

Noncontact AFM imaging was used as an alternative technique to investigate the topography of porous and 'fully-hardened' Ebonex®. Pore shapes were significantly less affected by the profile of the tip than those imaged using contact mode. The surface of the porous tile also appeared rougher than that obtained with contact mode imaging. This supports the suggestion that undesirable tip-sample interactions cause Ebonex® particles to be displaced by the scanning tip during contact mode imaging.

STM images of porous and fully-hardened (nonporous) Ebonex® tiles are shown in Fig. 3(a) and (b), respectively. These images are noticably different to those obtained by contact and noncontact mode AFM. The pores in the porous tile are much less affected by tip geometry and, as with noncontact AFM studies, the surface had a granular appearance. The fully-hardened tile exhibited a similar roughness to the porous tile ($R_a$: $14 \pm 7$ nm cf. $17 \pm 6$ nm, respectively). Deep pores were not observed in this material, although small corrugations and voids of up to 300 nm deep were seen.

AFM studies of copper electrodeposition on Ebonex® were restricted to the porous Ebonex® material since it was of interest to see whether copper nucleation and early growth occurred largely in the pores or at other locations on the surface. Contact mode AFM imaging was chosen for the study since the Ebonex® surface appeared very smooth, for the reasons previously explained, and this would enable small growth centres of copper to be easily recognized.

Fig. 4(a) and (b) show AFM images of two different regions of a porous Ebonex® electrode on to which had been electrodeposited a nominal single monolayer of copper (sample C). Small crystallites of copper could easily be observed in the surface pores of the material. In Fig. 4(b), crystallites appear to completely fill one of the pores and further growth is observed on the flat region outside the pore. Nucleation of copper within pores would be expected to occur, since these sites are more energetically favoured due to the greater number of dislocations, which 'seed' the nucleation and further growth of the copper deposit.

For thicker deposits of copper, passage of a charge equivalent to a nominal coverage of 100 monolayers (sample D) resulted in observation of many crystallites on the flat surfaces of the electrode (Fig. 4(c) and (d)). Some of the larger crystallites (~ 1 $\mu$m) had a similar appearance to the pyramidal tip used to obtain the image. For this to occur, the crystalline deposit must have been much finer than the tip, and thereby contacting the side-walls of the probe during scanning. Such tip artefacts have been observed elsewhere [21]. These artefacts became larger with increasing film thickness and little information could be obtained from such images.

## 4. Conclusions

The topography of porous and fully-hardened (nonporous) Ebonex® electrodes has been investigated by atomic force microscopy (AFM) and scanning tunnelling microscopy (STM). The surface porosity of these electrodes is known to have a marked affect on their electrochemical properties. The porous material was found to have a porosity in the range of 12% to

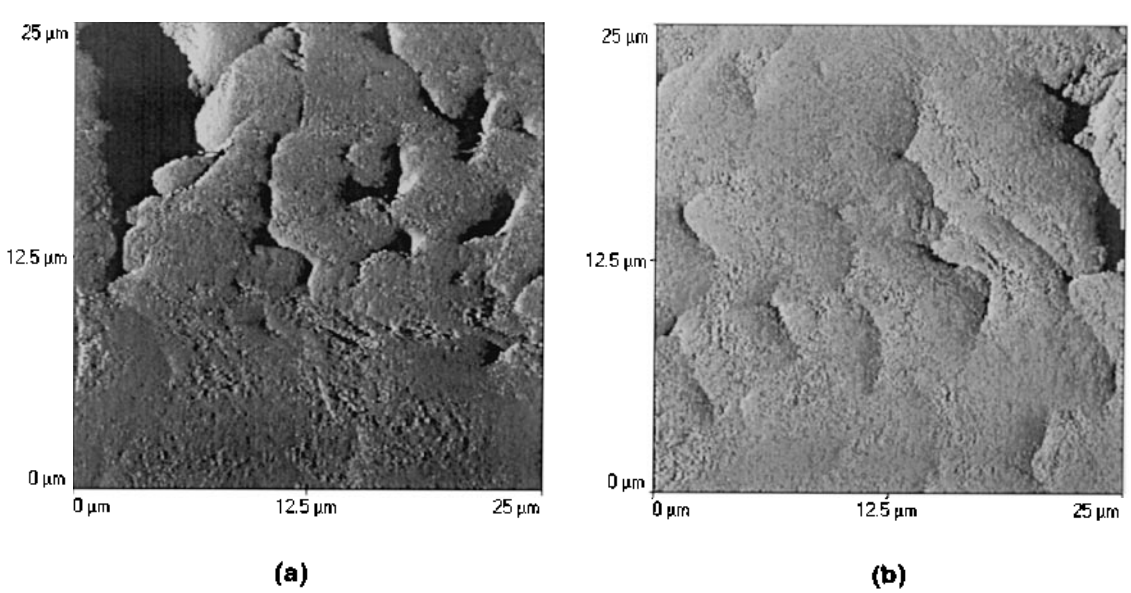


Fig. 3. STM (constant current mode) images of (a) porous and (b) 'fully-hardened' (nonporous) Ebonex® obtained using an electrochemically etched tungsten tip. Tip bias potential 5 mV (sample 0 V), tunnelling current 1.0 nA, scan rate 40 $\mu$m s$^{-1}$.

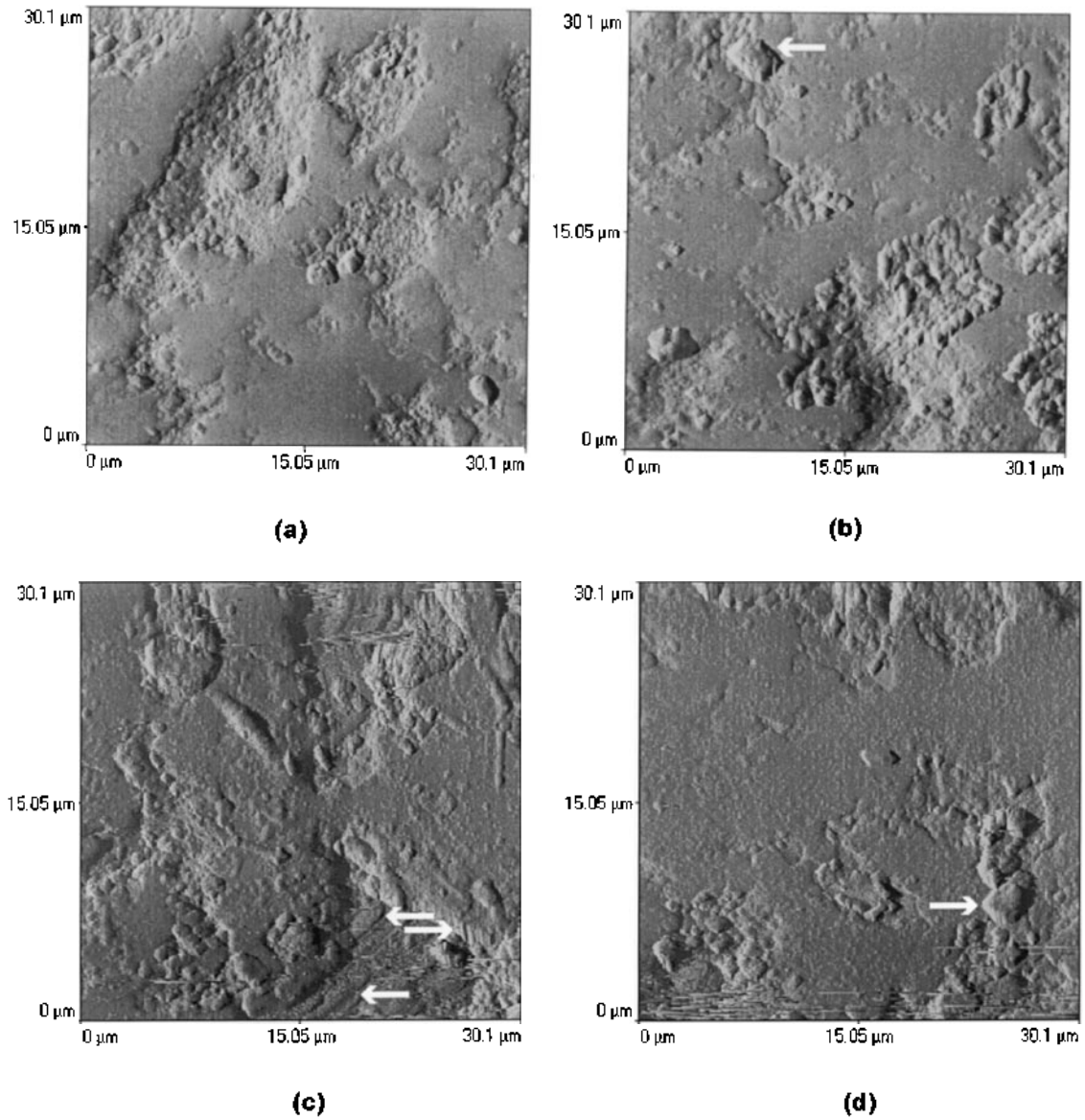


Fig. 4. AFM (contact mode) images of porous Ebonex® on to which (a–b) a nominal single monolayer, and (c–d) a nominal coverage of 100 monolayers of copper had been electrochemically deposited. Scan rate 75 $\mu$m s$^{-1}$. Arrows show locations of artefacts caused by the sidewalls of the pyramidal tip contacting large copper crystallites.

15%, and that for the fully-hardened material, 1% to 2%. AFM provides a rapid and useful technique for qualitative and quantitative characterization of Ebonex® electrodes. A direct measure of surface porosity can be obtained, which is more significant than the bulk porosity values determined from water immersion techniques. AFM also provides line profiles of surfaces and surface roughness data can be easily obtained. Nucleation and initial growth of copper on Ebonex® was seen to occur preferentially in the surface pores of the material, as might be expected from energetic considerations. Topographic images were found to be affected by tip geometry. For AFM contact methods, artefacts of similar dimensions to the scanning tip were seen for surface features possessing edges steeper than 45°. Hence, noncontact AFM and STM are better methods for imaging these materials.

## Acknowledgements

A. H. Nahlé wishes to thank the American University of Beirut for study leave. The authors are grateful to K. Ellis (Atraverda) and D. Brackenbury (EDA) who supplied Ebonex® samples.

## References

[1] A. Magnéli, S. Anderson, B. Collen and U. Kuylenstierna, *Acta Chem. Scand.* **11** (1957) 1641.
[2] R. R. Miller-Folk, R. E. Noftle and D. Pletcher, *J. Electroanal. Chem.* **274** (1989) 257.
[3] J. E. Graves, D. Pletcher, R. L. Clarke and F. C. Walsh, *J. Appl. Electrochem.* **21** (1991) 848.
[4] J. E. Graves, D. Pletcher, R. L. Clarke and F. C. Walsh, *J. Appl. Electrochem.* **22** (1992) 200.
[5] K. Kolbrecka and J. Przyluski, *Electrochim. Acta.* **39** (1994) 1591.
[6] R. L. Clarke and S. K. Harnsberger, *Am. Lab.* **20** (N6A) (1988) 8–10.

[7] R. L. Clarke, *in* 'Proceedings of the Second International Forum of Electrolysis in the Chemical Industry', Deerfield Beech, Fl (1988).
[8] P. C. S. Hayfield and R. L. Clarke, The electrochemical characteristics and uses of Magnéli phase titanium oxide ceramic electrodes, Electrochemical Society Spring Meeting, Los Angeles, 7–12 May (1989).
[9] S. Y. Park, S. I. Mho, E. O. Chi, Y. U. Kwon and I. H. Yeo, *Bull. Korean Chem. Soc.* **16** (1995) 82.
[10] C. L. K. Tennakoon, R. C. Bhardwaj and J. O. Bockris, *Int. J. Hydrogen Energy*, **19** (1984) 23.
[11] L. He, H. F. Franzen, J. E. Vitt and D. C. Johnson, *J. Electrochem. Soc.* **141** (1994) 1014.
[12] R. J. Pollock, J. F. Houlihan, A. N. Bain and B. S. Coryea, *Mat. Res. Bull.* **19** (1984) 17.
[13] G. Binnig, H. Rohrer, C. Gerber and E. Heibel, *Appl. Phys. Lett.* **40** (1982) 178.
[14] G. Binnig, C. F. Quate and C. Gerber, *Phys. Rev. Lett.* **59** (1986) 930.
[15] D. A. Bonnell, 'Scanning Tunnelling Microscopy and Spectroscopy' VCH, New York (1993).
[16] J. P. Ibe, P. P. Bey, Jr., S. L. Brandow, R. A. Brizzola, N. A. Burnham, D. P. DiLella, K. P. Lee, C. R. K. Marrian and R. J. Colton, *J. Vac. Sci. Technol.* **A8** (1990) 3570.
[17] TopoMetrix SPM Lab., Version 3.06.06, TopoMetrix Corporation, Santa Clara, CA, USA (1996).
[18] P. Dietz, P. K. Hansma, O. Inacker, H. D. Lehmann and K. H. Herrmann, *J. Membrane Sci.* **65** (1992) 101.
[19] BS. EN. 623-2 'Advanced Technical Ceramics – Monolithic Ceramics – General and Textural Properties. Part 2: Determination of Density and Porosity', Sept. 1993.
[20] K. Ellis, Atraverda Ltd, Sheffield, UK, personal communication.
[21] T. O. Glasbey, G. N. Batts, M. C. Davies, D. E. Jackson, C. V. Nicholas, M. D. Purbrick, C. J. Roberts, S. J. B. Tendler and P. M. Williams, *Surf. Sci.* **318** (1994) L1219.